Cell Reports, Volume *44*

Supplemental information

Uncovering the mechanism for polar sequestration of the major bacterial sugar regulator by high-throughput screens and 3D interaction modeling

Nitsan Albocher-Kedem, Meta Heidenreich, Amir Fadel, Elizabeta Sirotkin, Omer Goldberger, Anat Nussbaum-Shochat, Emmanuel D. Levy, Ora Schueler-Furman, Maya Schuldiner, and Orna Amster-Choder

Fig. S1. Screening for EI functional but diffused mutants.

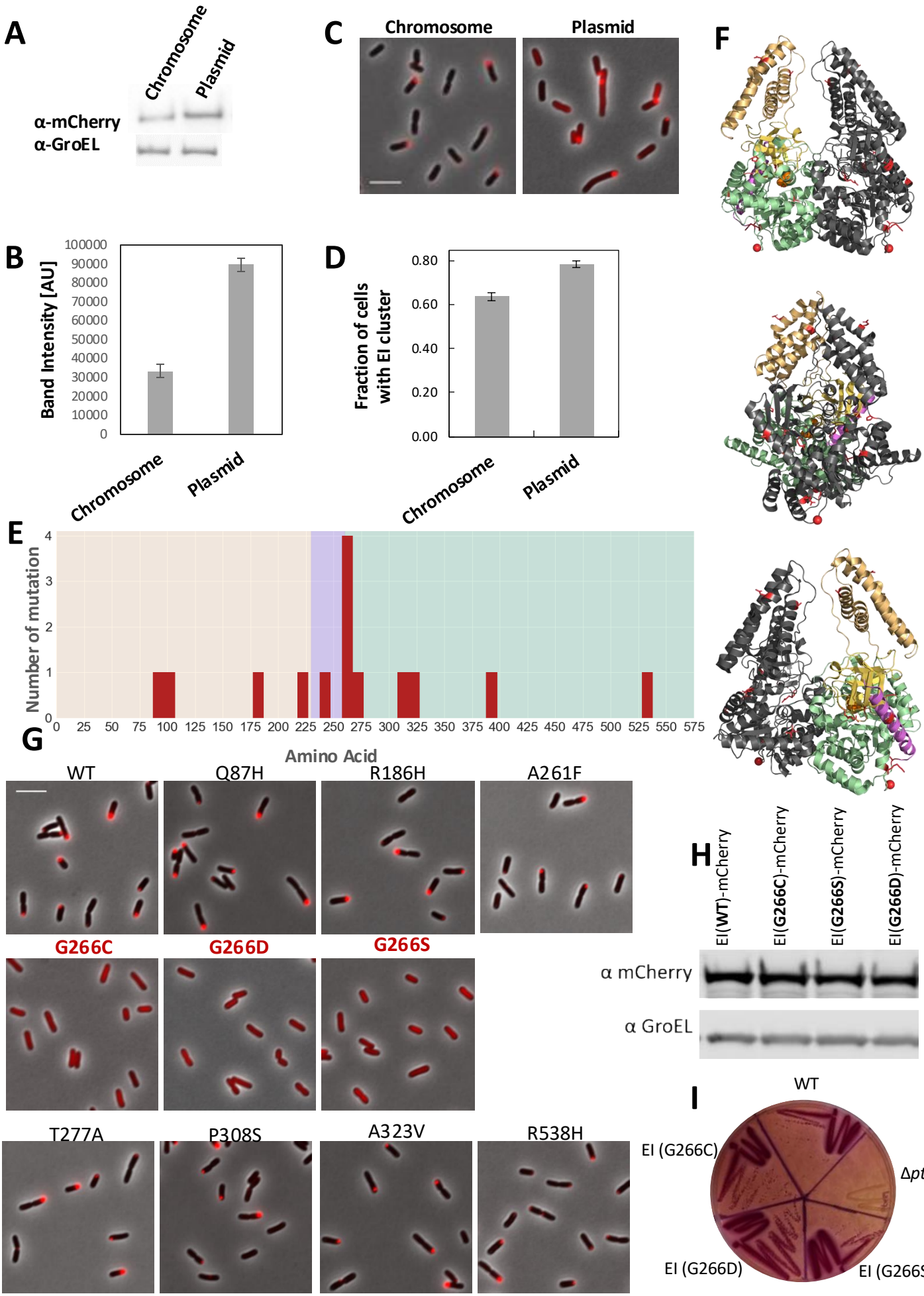

(A) Comparing the level of EI-mCherry expressed from the chromosomal *pts* promoter and locus or from a low copy plasmid that carries the *pts* operon with its native promoter by Western blot analysis. The EI-mCherry and GroEL were detected by α-mCherry α-GroEL antibodies, respectively.

(B) The level of EI-mCherry in (A) normalized to the level of GroEL.. Error bars represent the standard deviations (SD) based on three biological replicates. Statistical analysis of the differences between the amount of protein was calculated by unpaired t-test *p*-value= 0.0029

(C) Representative images of cells expressing EI-mCherry from the plasmid and the chromosome. Scale bar, 2 µm.

(D) The fraction of cells expressing EI-mCherry from the plasmid and the chromosome with clusters of EI-mCherry (n=790). The bars represent the SD based on five fields. Statistical analysis of the differences between the number of cells with an EI cluster was calculated by unpaired t-test *p*-value= 0.027.

(E) A histogram showing the position of the amino acids that were substituted in EI and the number of times that they came up in the screen for EI functional mutants that do not cluster with TmaR. An orange background marks the N-terminal domain of EI, purple background marks its linker region, and green background marks its C-terminal domain.

(F) The 3D structure of the EI dimer (protein data bank (PDB) id 2HWG). The models are cartoons showing the EI 3D structure from different angles. One subunit of EI dimer is colored in grey. In the other subunit, EIN is colored in orange, the linker region in purple and EIC in green. Amino acids whose substitution yielded functional but mislocalized EI mutants are marked in red. G266 in both subunits is presented as a red sphere.

(G) Representative images of cells expressing mCherry-tagged (red) WT EI or one of its variants with a single amino acid substitution from the chromosome native promoter and locus. Scale bar, 2 µm.

(H) Western blot analysis showing the level of EI-mCherry and of GroEL, detected by α-mCherry α-GroEL antibodies, respectively, in cells expressing mCherry-tagged wild type EI (WT) or one of the three EI-G266 mutants from the native *pts* promoter and locus in the chromosome.

(I) Testing the effect of EI G266 mutations on EI function. A representative MacConkey plate supplemented with 0.4% glucose. Red color indicates sugar consumption and, hence, that EI is functional. Cells expressing mCherry-tagged WT EI or one of the three EI-G266 mutants from the native *pts* promoter and locus in the chromosome were streaked on the plate. Cells deleted for the *ptsI* gene, which encodes EI (Δ*ptsI*), grow as white colonies, providing a negative control.

Fig. S2. 3D structures of EI obtained by X-ray crystallography and NMR

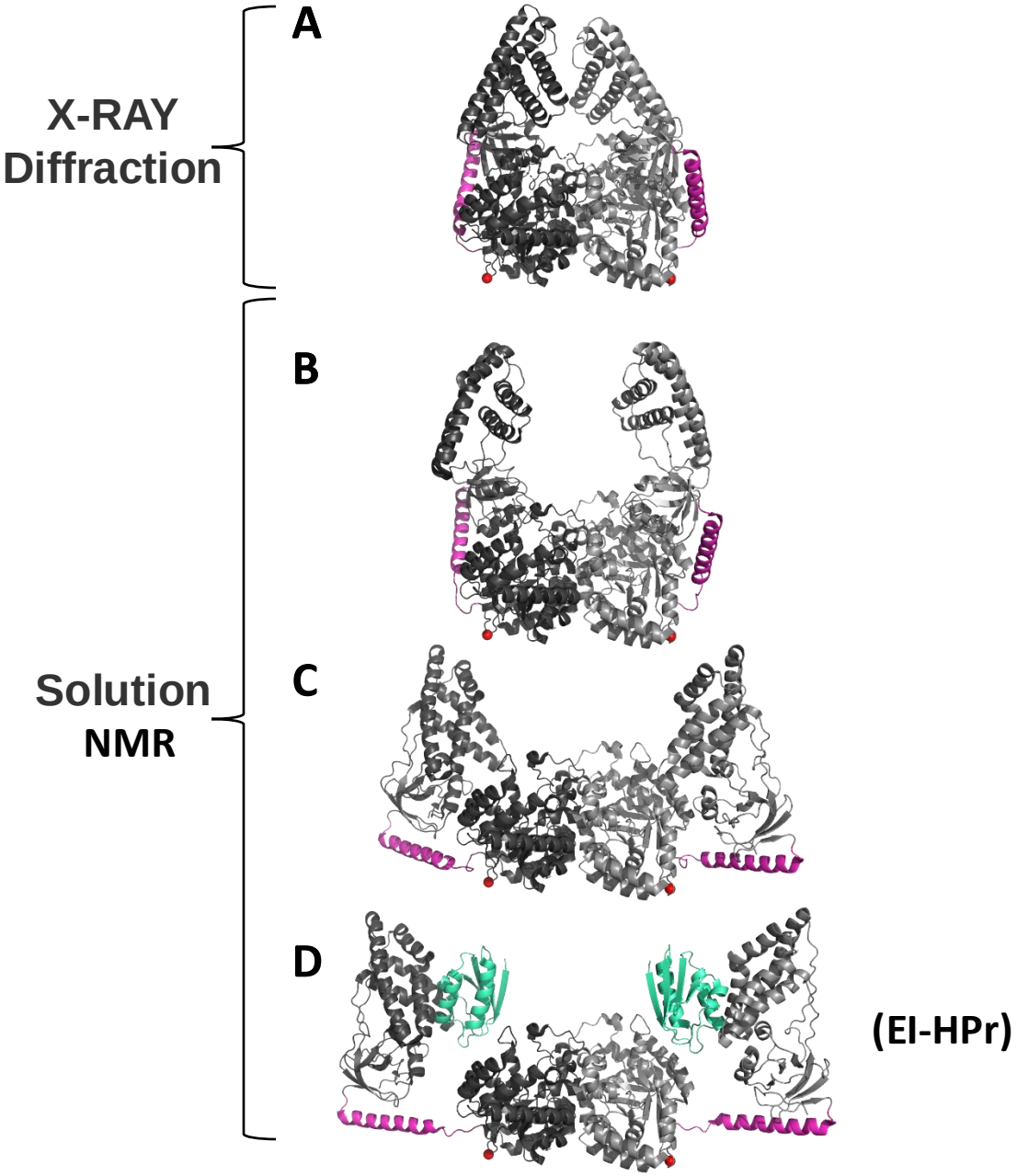

Shown are 3D structures of EI dimer obtained by X-ray or NMR (as indicated on the left): (A) An X-ray solution of EI structure (PDB ID: 2HWG). (B) Closed NMR structure (PDB ID: 2N5T). (C) Open structure of EI obtained by NMR (PDB ID: 2KX9). (D) Open structure of EI bound to HPr obtained by NMR (PDB ID: 2XDF). EI is in shades of grey, the linker is colored in magenta, G266 is marked as a red sphere, HPr is in cyan.

Fig. S3. The interplay between EI-G266 mutants and TmaR

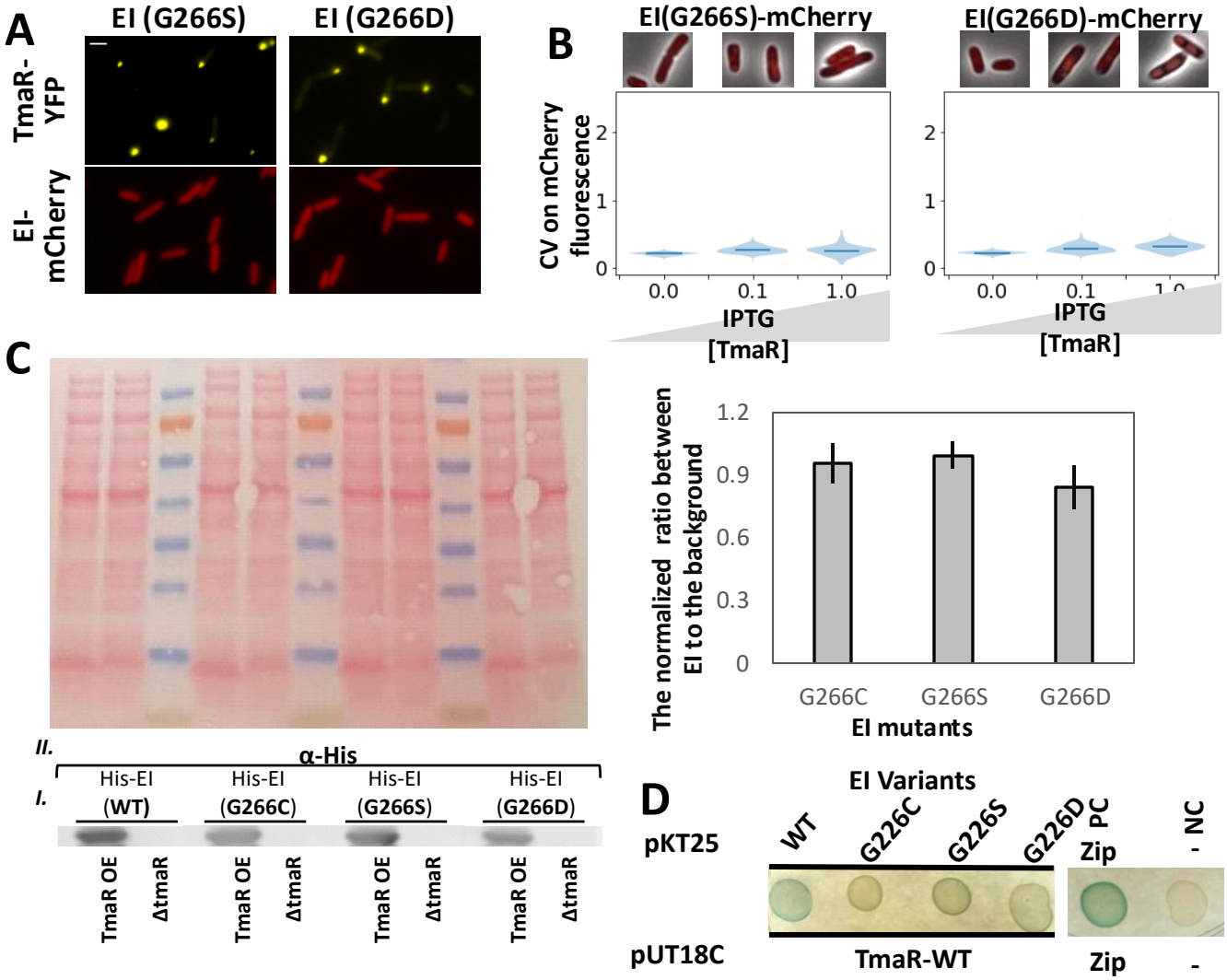

(A) Images of cells expressing TmaR-YFP (yellow) and mCherry-tagged EI, G266S or G266D (red), all expressed from their respective native promoter and locus in the chromosome. Scale bars, 2 µm. (see the respective results with EI, WT and G226D in Fig. 1F).

(B) Cells expressing mCherry-tagged EI, G266S or G266D, from the native pts promoter and locus in the chromosome, and harboring a plasmid expressing TmaR from an IPTG-inducible promoter, grown with increasing concentrations of IPTG (0, 0.1 or 1 mM) were imaged. The Coefficient of Variance Intensity (CVI) of the respective EI variants throughout the cells were calculated. The lower panel shows images of the cells expressing the corresponding mCherry-tagged EI variants (red). The violin plots in the upper panel show the CVI of the corresponding mCherry-tagged EI variants. The blue lines show the medians (n is between 360-850 cells). Scale bars, 2 µm. (See the respective results with EI, WT and G266C in Fig. 1H)

(C) Far-Western analysis of the interaction between TmaR WT with either EI WT or one of EI G266 mutants. Left **Lower left panel**: Lysates of Δ*tmaR* cells overexpressing TmaR or not expressing TmaR were fractionated by SDS-PAGE, blotted onto four nitrocellulose membranes and probed with either purified His-tagged WT EI or one of the EI mutants (I) followed by anti-His tag antibody (II). The observed bands match TmaR size. **Upper left panel**: Shown is the membrane used for the Far-Western analysis stained with ponceau S to verify loading of equal amounts. **Right panel:** The column chart show the ratio between the band intensity of each His-tagged EI mutant and the background. The ratio obtained when WT TmaR and WT EI were co-expressed is defined as 1. The bars show the SDs between three biological replicates. Statistical analysis for the differences between WT and the mutants was conducted using the two-sided Mann-Whitney test, which was non-significant.

(D) Representative results obtained with the bacterial two-hybrid assay, which tested the interaction of WT TmaR with either WT EI or the EI mutants with the indicated replacements of G266. The interaction between two leucine zipper region of the GCN4 yeast protein (Zip) served as a positive control (PC) for an interaction. A plasmid not expressing any TmaR variant unfused T18 and T25 served as a negative control (NC). The different proteins were expressed from pUT18C or pKT25, as indicated.

Fig. S4. Screening TmaR mutants that fail to recruit EI to the poles

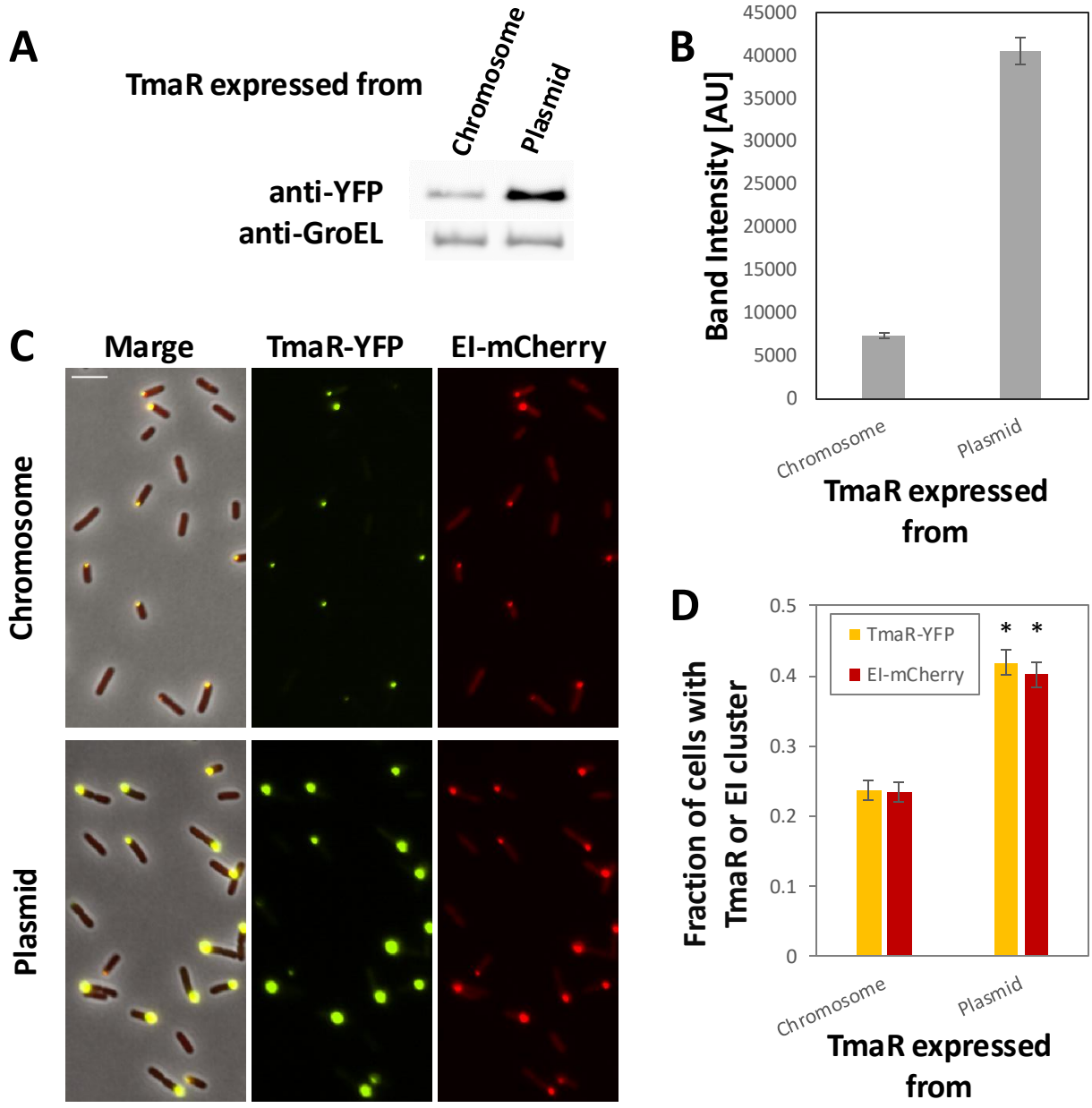

(A) Western blot analysis showing the level of TmaR-YFP expressed from the native *tmaR* promoter and locus either from the chromosome or from a low copy plasmid. The cells also express EI-mCherry from its native promoter and locus. TmaR-YFP and GroEL were detected by α-YFP and α-GroEL antibodies, respectively.

(B) The level of TmaR-YFP in (A) normalized to the level of GroEL. Error bars represent (SD) based on four biological replicates. Statistical analysis of the differences between the amount of protein calculated by unpaired t-test *p*-value=0.0013

(C) Representative images of cells expressing TmaR-YFP (yellow) from the native *tmaR* promoter and locus either from the chromosome or from a low copy plasmid, as well as EI-mCherry expressed from the chromosome (red). Scale bars, 5 µm.

(D) Fraction of cells with clusters of TmaR-YFP (yellow bares) and EI-mCherry (red bares) in the background described in C (n=458). Error bars represent the SD based on five fields. Statistical analysis of the differences between the number of cells with a TmaR or an EI cluster was calculated by unpaired t-test. *<0.0001.

Fig. S5. EI is not recruited to the poles by the screen-isolated TmaR mutants

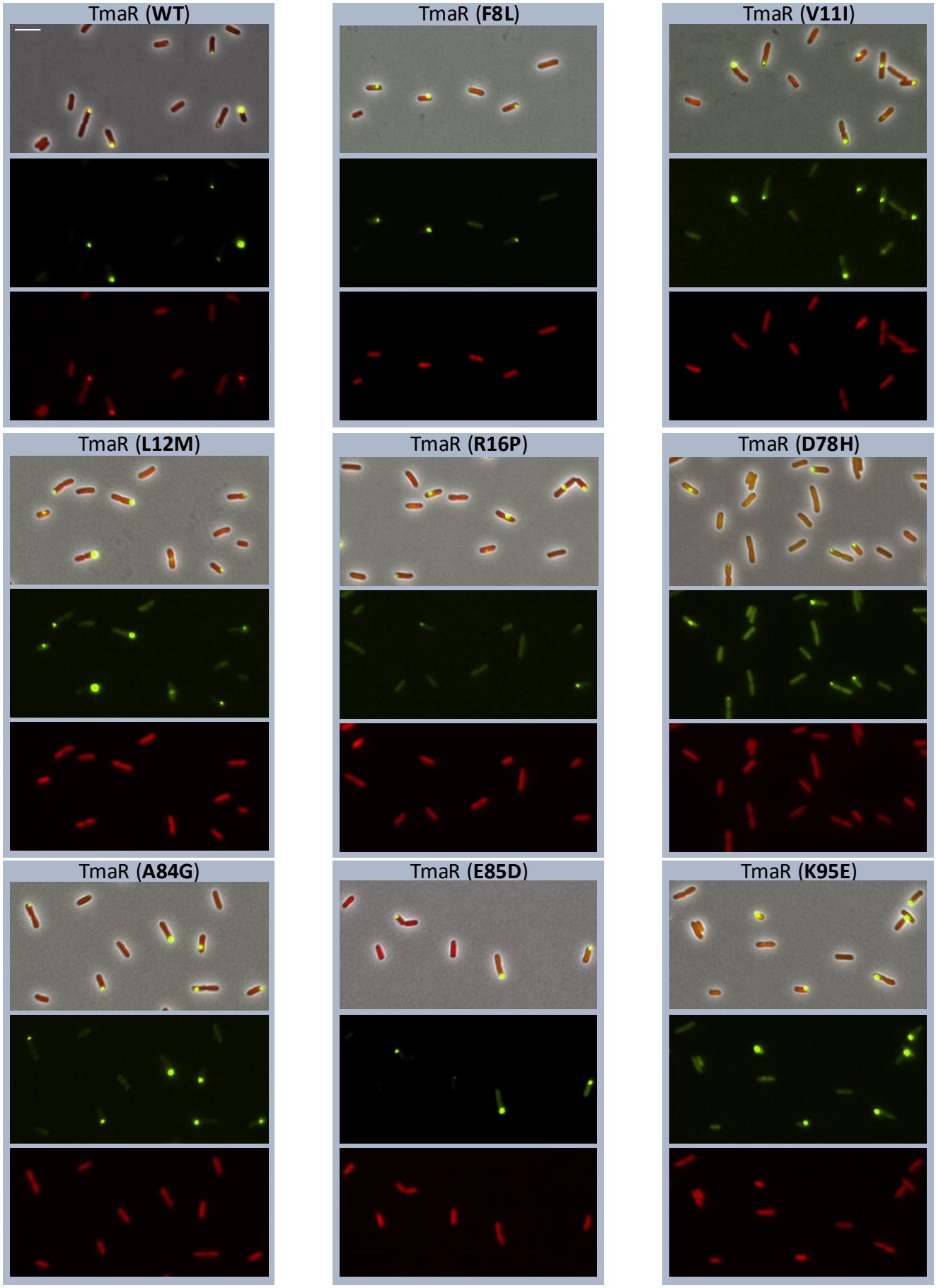

Representative images of cells expressing WT EI-mCherry (red) and YFP-tagged WT TmaR or one of its variants with a single amino acid substitution (yellow) from their respective chromosomal native promoter and locus. Scale bar, 5 µm.

Fig. S6. Further characterization of the TmaR mutants that fail to recruit EI

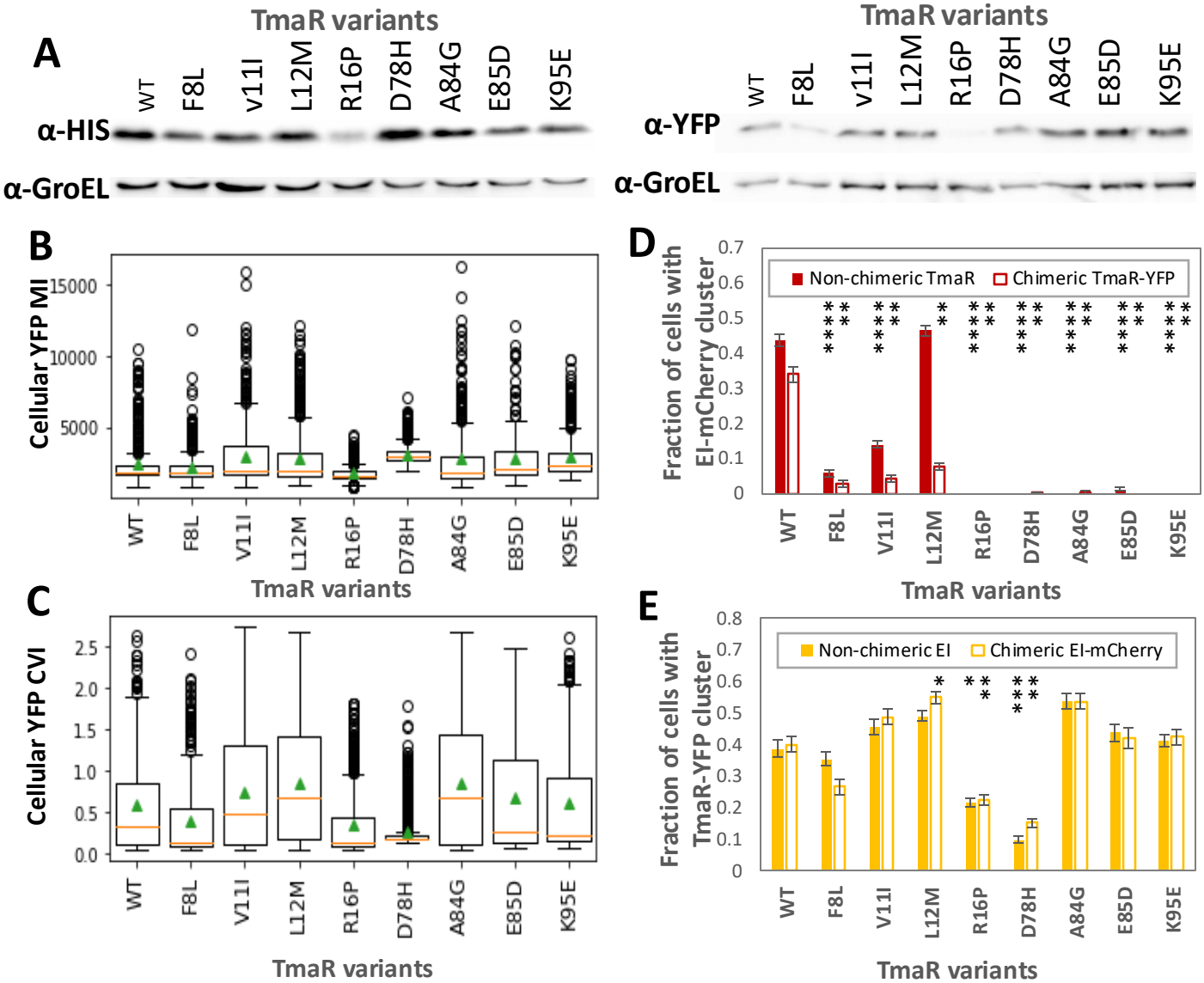

(A) Western blot analysis showing the level of HIS-tagged (left) and YFP-tagged (right) TmaR WT or one of its variants, all expressed from the native *tmaR* promoter and locus in the chromosome. The YFP-tagged TmaR variants and GroEL were detected by α-YFP and α-GroEL antibodies, respectively.

(B) Box plot showing mean intensity (MI) of the YFP signals calculated for cells expressing YFP-tagged WT TmaR or one of its mutants, all expressed from the native *tmaR* promoter and locus in the chromosome (n is between 404 and 812 cells).

(C) Box plot showing the coefficient of variation Intensity (CVI) of the YFP signals calculated for cells expressing YFP-tagged WT TmaR or one of its mutants, all expressed from the native *tmaR* promoter and locus in the chromosome (n is between 404 and 812 cells).

(D) Comparison of fraction of cells with clusters of EI-mCherry in a population expressing untagged (solid red column) or YFP-tagged (hollow red column) WT or mutant TmaR proteins. All proteins were expressed from their native promoter and locus in the chromosome. The bars show the SDs (n is between 404 and 812 cells). Statistical analysis of the differences between mutants and WT was calculated for cells in 10 fields by unpaired t-test **<0.0001, ****<10^{-10}, NS>0.01.

(E) Comparison of the fraction of cells with clusters of YFP-tagged WT or mutant TmaR proteins in a population expressing untagged EI (solid yellow columns) or EI-mCherry (hollow yellow column). All proteins were expressed from their native promoter and locus in the chromosome. The bars show the SDs (n is between 404 and 812 cells). Statistical analysis of the differences between mutants and WT was calculated for cells in 10 fields by unpaired t-test *<0.001, **<0.0001, ***<10^{-5}, NS>0.01.

Fig. S7. EI-mCherry localization in cells expressing the various His-tagged TmaR variants from a plasmid

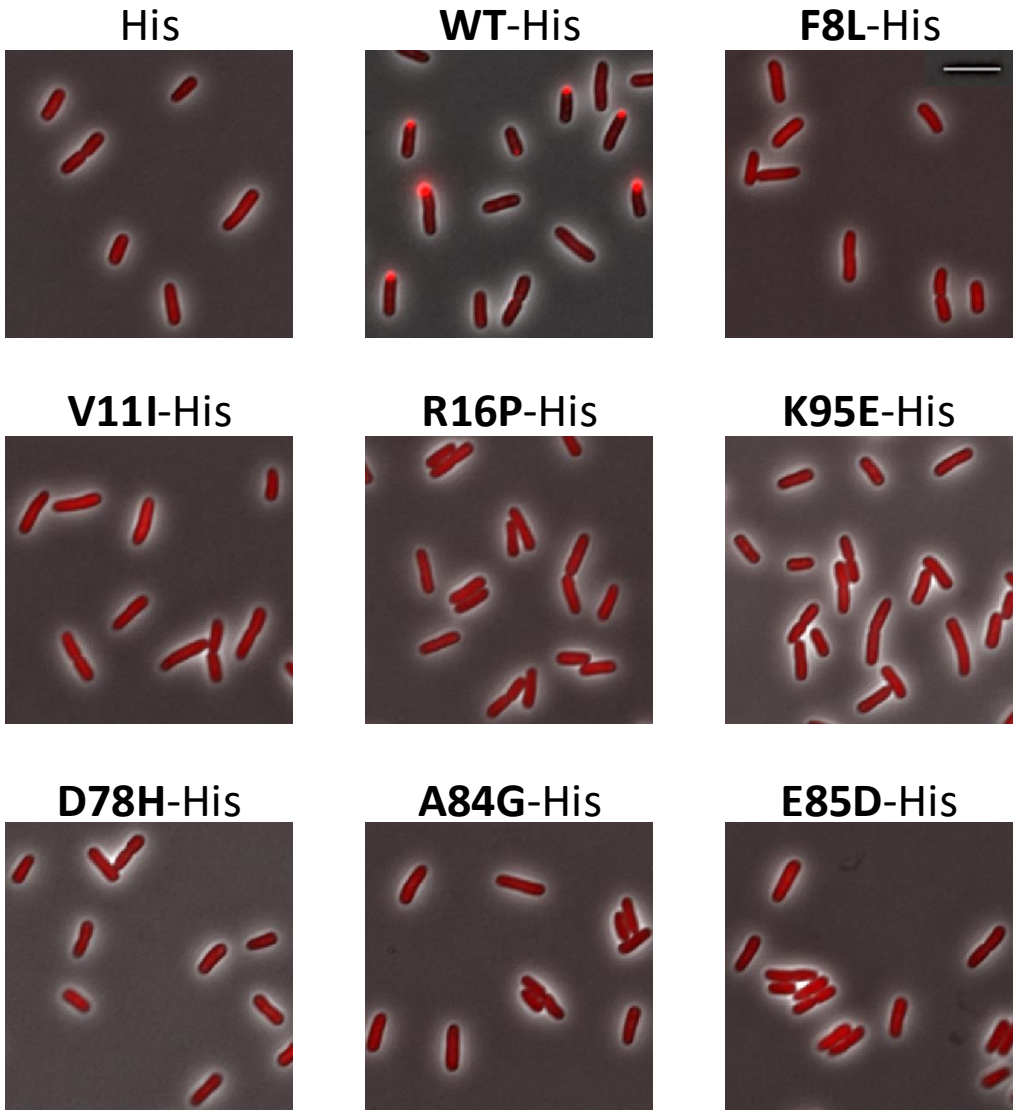

Representative images of Δ*tmaR* cells expressing EI-mCherry from the *pts* native promoter and locus in the chromosome and harboring a plasmid expressing one of the His-tagged TmaR variants or just the His-tag. Scale bar, 2 µm.

Fig. S8. The interaction between WT EI and TmaR variants tested by a bacterial two-hybrid assay

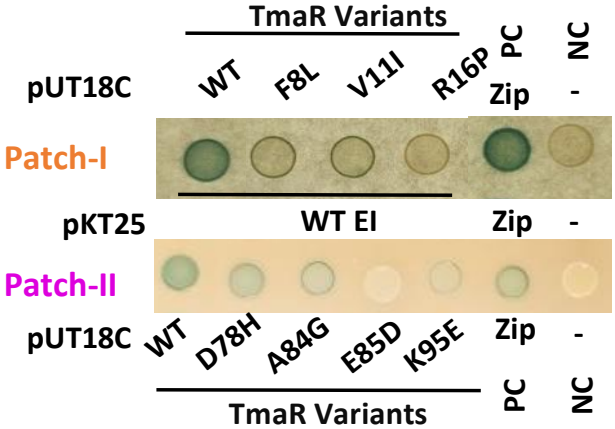

Representative results obtained with the bacterial two-hybrid assay, which tested the interaction of WT EI fused to T25 with either WT TmaR or the different TmaR mutants with the indicated point mutations fused to T18. The interaction between two leucine zipper region of the GCN4 yeast protein (Zip) served as a positive control (PC) for an interaction. A plasmid not expressing any TmaR variant unfused T18 and T25 served as a negative control (NC). The different proteins were expressed from pUT18C or pKT25, as indicated.

Fig. S9. Localization of WT and mutant EI and TmaR proteins in yeast cells

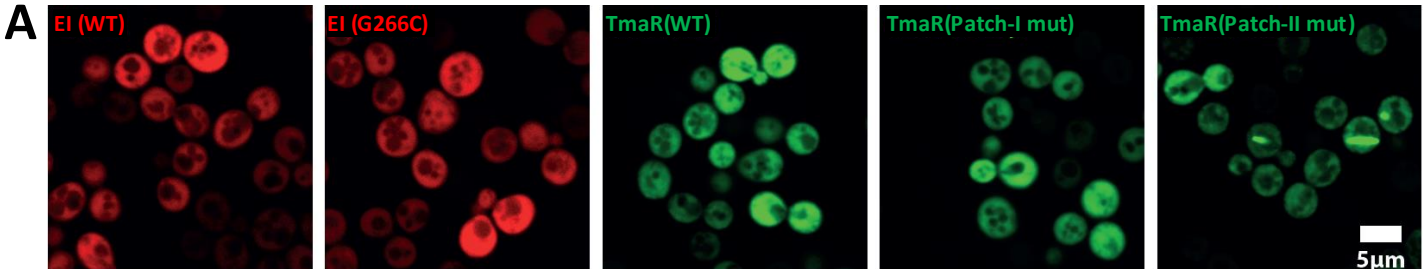

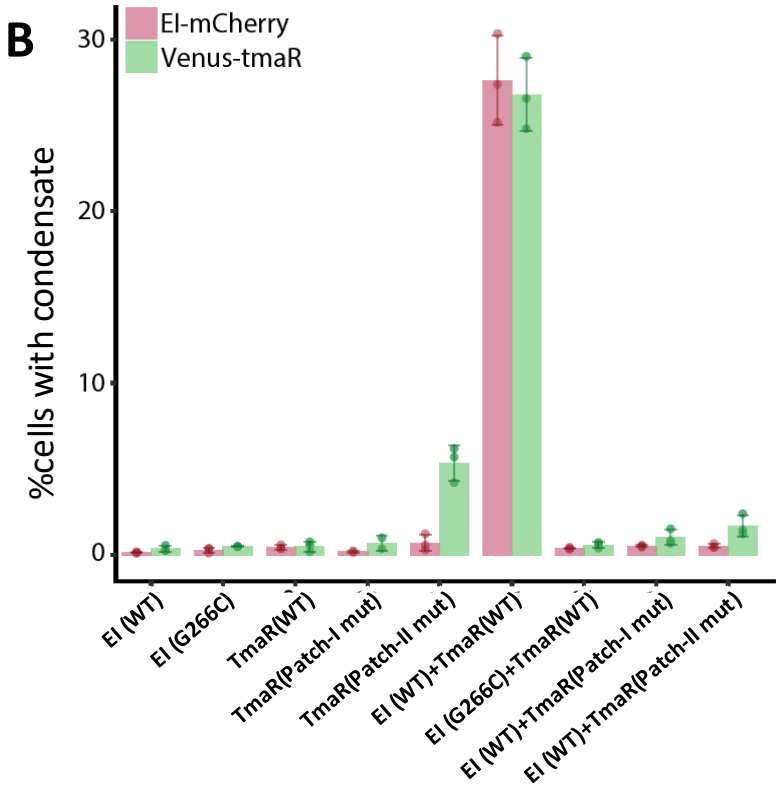

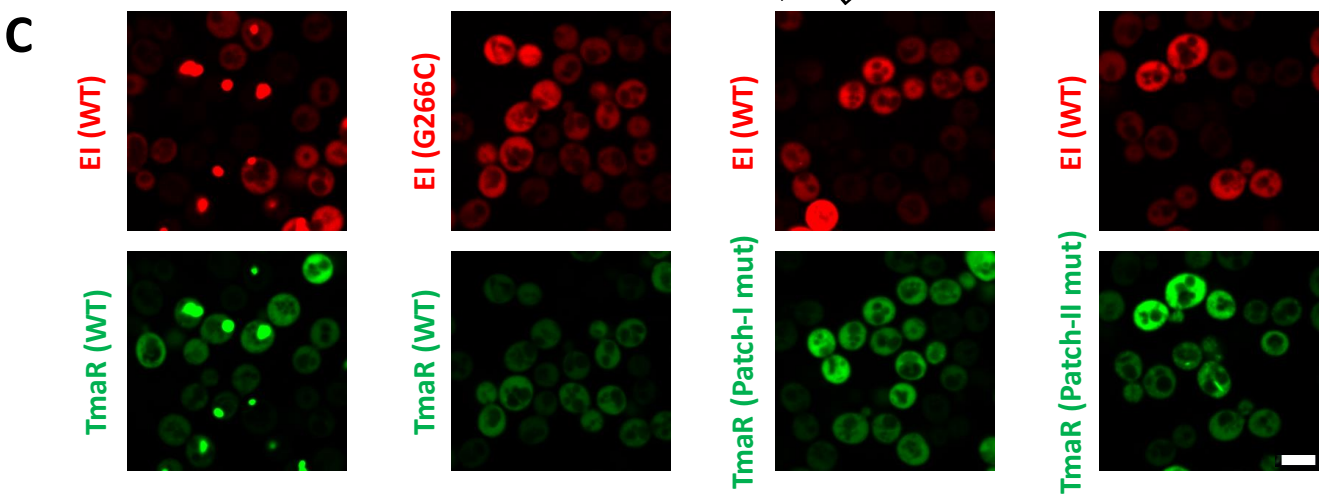

(A) Images of yeast cells expressing a single *E.coli* protein. From left to right: EI(wt), EI(WT)-mCherry; EI(G266C), EI(G266C)-mCherry; tmaR(wt), Venus-TmaR(WT); tmaR(patch-I mut), Venus-TmaR(F8L, V11I, R16P); and tmaR(patch-II mut), Venus-TmaR(D87H, A84G, E85D). Scale bars, 5 μm.

(B) A bar plot showing the percentage of cells with condensate. Points represent biological replicates with each strain; the bar height indicates the mean and error bars show one standard deviation.

(C) Shown are the separate RFP (EI variants) and GFP (TmaR variants) channels of the yeast cell images, which express both EI and TmaR variants, shown in Fig. 3C as merged. Scale bars, 5 μm.

Fig. S10: Models of the EI-TmaR interaction generated by ClusPro docking

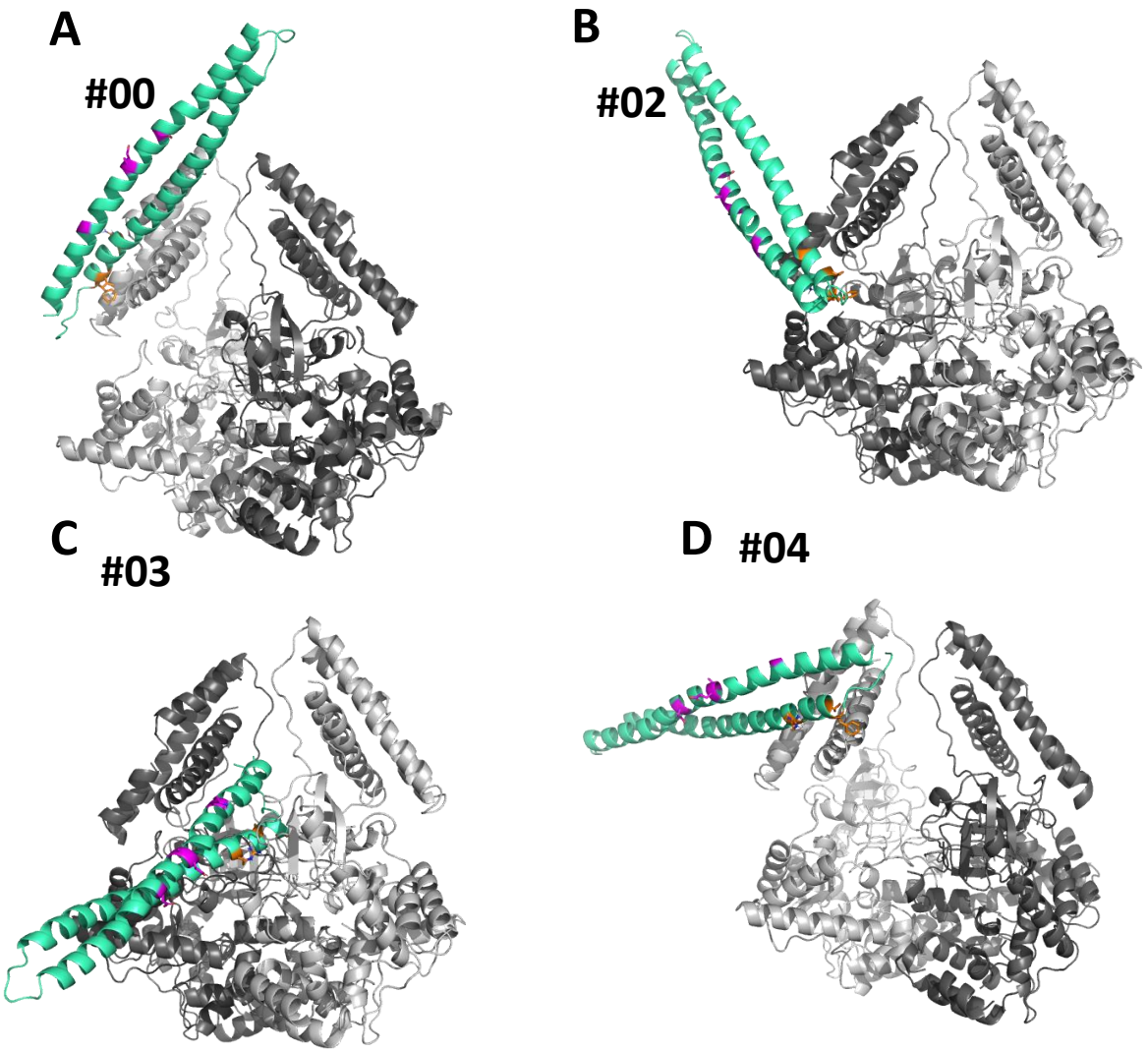

The top models for an EI-TmaR complex obtained by docking the solved structure of the EI dimer (PDB id 2HWG; see Fig. 1E) and a structural model of TmaR (generated using trRosetta; see Fig. 3C) using ClusPro. TmaR is shown in green-cyan, with the residues in the sticky and stabilizing patches substituted in the mutants obtained in our screen colored in orange and magenta, respectively, with their protruding side chains presented as sticks. Models #01 and #05 are a symmetric copy of models #00 and #3, respectively, and therefore not shown.

Fig. S11: Models of the EI-TmaR interaction generated by AlphaFold

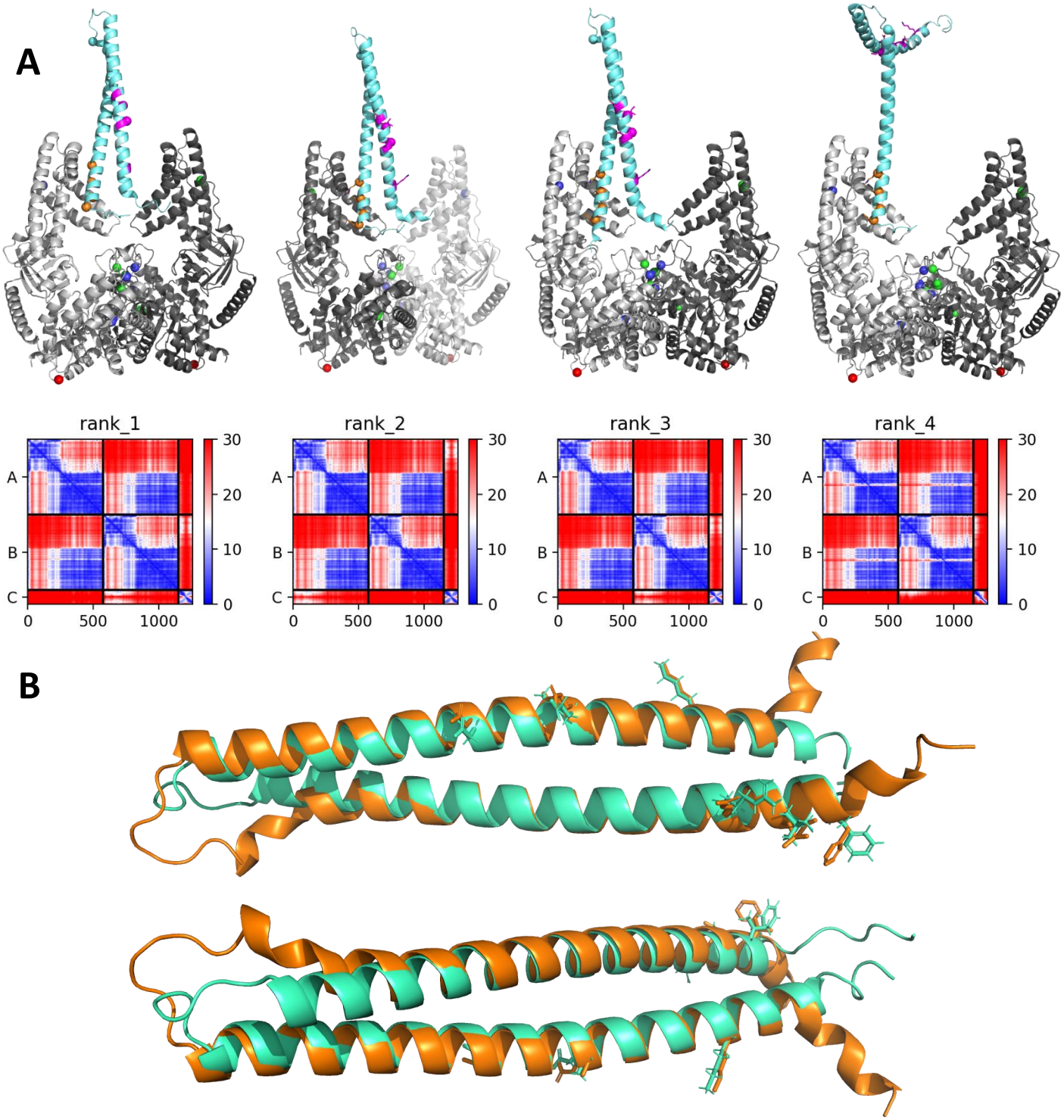

(A) **Top panel**: The four models for EI-TmaR complex obtained by AlphaFold. EI dimer is in shades of grey, with one subunit in dark grey and the other in light grey. The residues in EI and TmaR predicted by the RaptorX ComplexContact server to co-evolve with the highest scores (>0.3) are presented as spheres that are colored magenta in TmaR stabilizing patch, orange in TmaR sticky patch and blue and green in EI two subunits, respectively. **Lower panel**: the PAE plots of each model.

(B) Overlay of TmaR predicted structures by trRosseta (cyan) and AlphaFold (orange). The AlphaFold structure was generated with AlphaFold multimer, taken from the top ranked EI-TmaR complex (shown in A). The amino acids that came up in our screen are presented as sticks.

Fig. S12: Residue in EI and TmaR predicted to interact electrostatically

Sticky patch

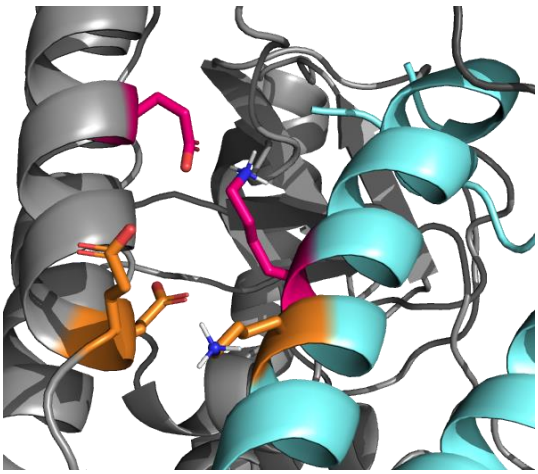

Stabilizing patch

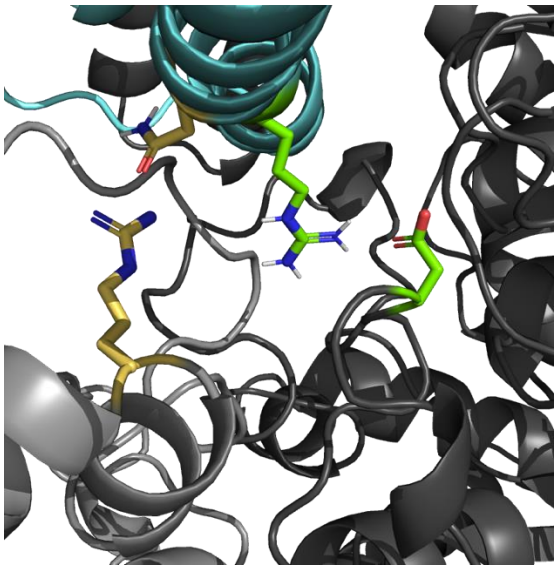

EI	TmaR
E109	R98
E116,E117	R95
R366	N22
D468	R19

Shown are four pairs of residues that are predicted to interact electrostatically in EI and TmaR. Two residues in each patch of TmaR were selected. Each pair is colored in a unique color and the residues appear as sticks in the respective color in the 3D model.

Fig. S13: Conservation of the putative interacting residues in EI and TmaR

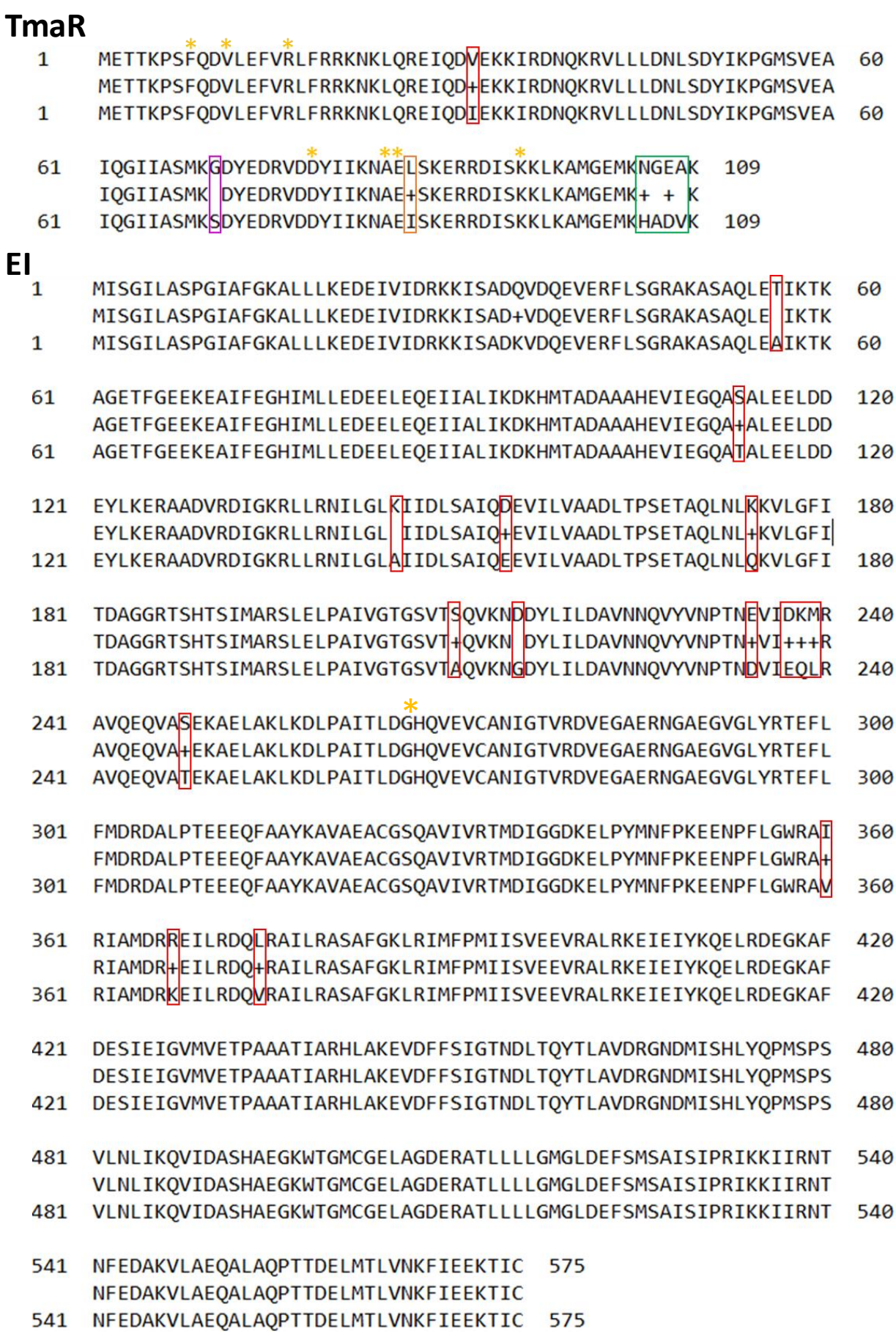

Sequence alignments of TmaR and EI proteins from *E. coli* (top row) and *S. typhimurium* (bottom row). Boxes mark the residues that are different in the two species. Yellow stars mark the residues that were mutated in our screens.

Fig. S14: Models for EI interaction with HPr or TmaR

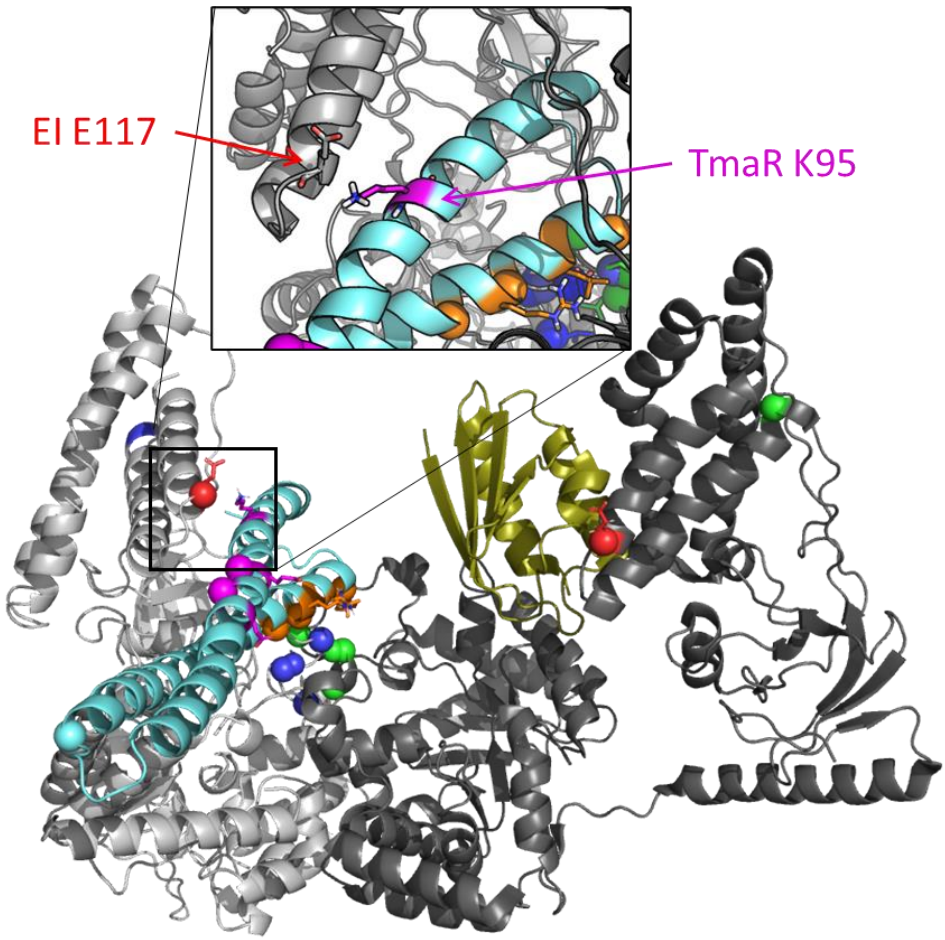

The interaction between E117 in EI and K95 in TmaR is predicted to stabilize the closed conformation of EI. Shown is an interaction model between TmaR and a hybrid 3D structure of EI dimer composed of one closed and one open conformation. The left subunit (light gray) is from the close conformation structure (PDB id 2HWG), whereas the right subunit (dark gray) is from the open conformation structure. HPr-bound conformation (PDB id 2XDF) is in deep olive green; TmaR is in cyan, with the residues in the sticky and stabilizing patches, which were substituted in the mutants obtained in our screen, colored in orange and magenta, respectively, with their protruding side chains presented as sticks. The E117 residue in EI, which is in close proximity to K95 in TmaR, is marked as a red sphere with its protruding side chains presented as sticks in both EI subunits. The residues in EI and TmaR predicted by RaptorX ComplexContact to coevolve with the highest scores (>0.3) are presented as spheres - magenta and orange in the stabilizing and sticky patches on TmaR, respectively, and blue and green in the two EI subunits, respectively. Note the interactions formed by E117 of EI with TmaR in the closed conformation (in the enlargement), and with HPr in the open conformation.

Supplemental Tables

Tables

Table S1: EI mutants isolated by a screen for functional EI variants that do not cluster with TmaR
Each row gives the information for one EI mutant.

Mutant number	Number of mutations that alter the protein sequence	The mutations at the DNA level	The mutations at the protein level
1	2	G557A : G796A	R186H : G266S
2	5	G261T : C665T : G721A : C968T : G1613A	Q87H : A222V : A241T : A323V : R538H
3	1	G796T	G266C
4	1	G495A : G797A	P165P : G266D
5	4	G304A : C782T : C830T : C922T	A102T : A261F : T277A : P308S
6	1	A1177T	I393F

Table S2: Mutants isolated by a screen for TmaR variants that fail to recruit EI to the poles
Each row gives the information for one TmaR mutant.

Mutant number	Number of mutations that alter the protein sequence	The mutations on the DNA level	The mutations on the protein level
1	2	T22C	F8L
2	2	C24A ; C201G	F8L ; S67R
3	1	G31A	V11I
4	1	G31A	V11I
5	1	G31A	V11I
6	1	G31A : G79A	V11I: E27K
7	1	C34A	L12M
8	1	G47C	R16P
9	1	G47C	R16P
10	1	G47C	R16P
11	1	G47C	R16P
12	2	G47A ; A283G	R16P; K95E
13	1	G232C	D78H
14	1	G232C	D78H
15	1	C251G	A84G
16	1	G255T	E85D
17	1	A283G	K95E